All-fiber add/drop wavelength routing structure

Sumriddetchkajorn, Sarun, Riza, Nabeel

Sarun Sumriddetchkajorn, Nabeel A. Riza, "All-fiber add/drop wavelength routing structure," Proc. SPIE 4046, Advances in Optical Information Processing IX, (13 July 2000); doi: 10.1117/12.391939

SPIE.

Event: AeroSense 2000, 2000, Orlando, FL, United States

All-Fiber Add/Drop Wavelength Routing Structure

Sarun Sumriddetchkajorn and Nabeel A. Riza*

Photonic Information Processing Systems (PIPS) Laboratory
The School of Optics/Center for Research and Education in Optics and Lasers (CREOL)
University of Central Florida, 4000 Central Florida Blvd, Orlando, FL 32816-2700
Tel: 407-823-6829; Fax: 407-823-3354
E-mail: riza@creol.ucf.edu

ABSTRACT

A fiber-connectorized multiwavelength 2 × 2 switch structure is introduced for the first time that deploys a fiber loop mirror (FLM) arrangement with polarization control. Micromachine-based fiber squeezers that employ electrostatic actuation, magnetic actuation, and magnetic levitation and propulsion techniques are proposed for the implementation of a low-cost, high-speed, and compact polarization controller. Switch operation is achieved via a programmable waveplate effect rather than an optical power consuming long fiber loop length non-linear optical effect. The results from an experimental four-wavelength (i.e., 1546.92 nm, 1548.52 nm, 1550.12 nm, and 1551.72 nm) proof of concept switch using two mechanical fiber-based polarization controllers embedded in a short 7 m fiber loop indicates an average optical coherent crosstalk of -31.2 dB. Presently, optical loss is mainly limited by the WDM devices used in our experimental setup. Hence, without the WDM multiplexers, an average optical loss of 2.22 dB is measured over a 50 nm optical bandwidth. Also, an average 0.08 dB polarization dependent loss is measured for this broadband switch.

1. INTRODUCTION

Fiber optic switches (FOSs) are important for constructing flexible and reliable optical transmission and signal processing systems as they offer wide instantaneous bandwidths and immunity to electromagnetic interference in addition to eliminating the need for optical-to-electrical and electrical-to-optical conversion at the switching layer. Several FOSs approaches have been introduced over the years including FOSs based on opto-mechanical movement [1], nematic liquid crystals (NLCs) [2], ferroelectric liquid crystals (FLCs) [3], and microelectromechanical systems (MEMS) [4-5]. Opto-mechanical and MEMS-based switches utilize moving parts for switch operation, with fiber-to-fiber coupling through a MEMS structure. Switches based on NLCs and FLCs are perhaps not optimal for large scale cascaded network switching due to the polarization dependence of NLC and FLC materials. All these switches break the direct fiber-to-fiber connection to implement the switch mechanism, thus requiring careful optical alignment and packaging. Thus today most deployed components such as couplers, optical amplifiers, polarizers, optical attenuators, and wavelength filters used in lightwave systems are fiber based devices that provide compactness and compatibility with fiber embedded systems. Moreover, these components can be easily connected to each other using either the fiber fusion splicing technique or fiber connectors. Hence, it would be desirable to have a fiber-connectorized multiwavelength 2 × 2 FOS for deployment in wavelength division multiplexed (WDM) fiber-optic communication systems.

One very useful all-fiber device is the fiber loop mirror (FLM) [6-7]. A variety of FLM-based systems have been demonstrated, including optical fiber sensors [8], optical logic gates [9], optical memories [10], optical phase conjugators [11], optical gain equalizers [12], wavelength multiplexers [13], wavelength converters [14], optical time division multiplexers [15], optical switches [16-17], and add-drop multiplexers [18]. In ref.18, one nonlinear loop mirror (NLM)-based switch acting as a self-synchronization unit and two NLM-based logic gates were used to demonstrate the add-drop operation, leading to a hardware complex system. In addition, although the earlier demonstrated optical switches based on the single nonlinear optical loop mirror offer fast switching speeds in the picoseconds domain, the switch functions only as an on-off shutter and is not the versatile 2 × 2 FOS required today for multiwavelength routing. There are also other limitations related to this nonlinear element (NLE) based shutter switch such as a low contrast ratio of < 21 dB, even when using a semiconductor optical amplifier as a NLE inside the loop. Without the NLE, a long length (e.g., > 1 km) of the standard single mode fiber (SMF) and a high power (e.g., hundreds of milliwatts) pump laser are required in this switch in order to

* Also with Nuonics, Inc., Orlando, FL, Tel: 407-963-3706; nriza@aol.com

In *Advances in Optical Information Processing IX*, Dennis R. Pape, Editor,
Proceedings of SPIE Vol. 4046 (2000) • 0277-786X/00/$15.00

obtain a sufficient nonlinear phase shift. Another disadvantage of using a long SMF to implement a FOS is the inherent dispersion effect of the fiber. This problem can be solved by using a dispersion shifted fiber (DSF) instead of the SMF, although at a much higher fiber cost (e.g., ~ 4 times/meter [19]). Furthermore, to perform the N-wavelength switching operation, the NLM-based switch [16] design for use in WDM communication systems requires either a high power tunable pump laser or N high power single wavelength lasers and a tunable wavelength filter to achieve a high crosstalk level. Another limiting factor of the NLM-based structures is that they are highly sensitive to acoustic disturbances. A long loop fiber will increase the acoustic noise sensitivity that will raise the bit error rate floor [20]. In addition, a NLM-based structure generally shows a high 5 dB polarization dependent loss (PDL) [21]. Several techniques such as the use of twisted fiber [21], cross spliced polarization maintaining DSF [22], and birefringent crystal [23] have been introduced in the NLM-based structure to achieve a low PDL of 0.5 dB. This PDL value is still higher than a PDL criteria (e.g., < 0.2 dB) required for the commercial 2 × 2 fiber-optic switch communication application [24].

With these issues in mind, this paper proposes to use an FLM arrangement that solves the problems inherent in the NLM-based switch to realize all-fiber multiwavelength 2 × 2 FOS [25-26]. Specifically, our 2 × 2 FOS operation is based on the combination of the retro-reflective optical structure and a phase shifter to control the well-known switch inversion characteristic of the fiber loop mirror. Key features of this switch includes short fiber lengths, all-fiber design, low loss, low optical power overhead, low optical coherent crosstalk, and low PDL. An experimental proof of concept 4-wavelength switch is demonstrated. System issues such as optical loss, optical coherent crosstalk, and PDL are discussed.

2. FLM-BASED ALL-FIBER MULTI-WAVELENGTH 2 × 2 FIBER-OPTIC SWITCH STRUCTURE

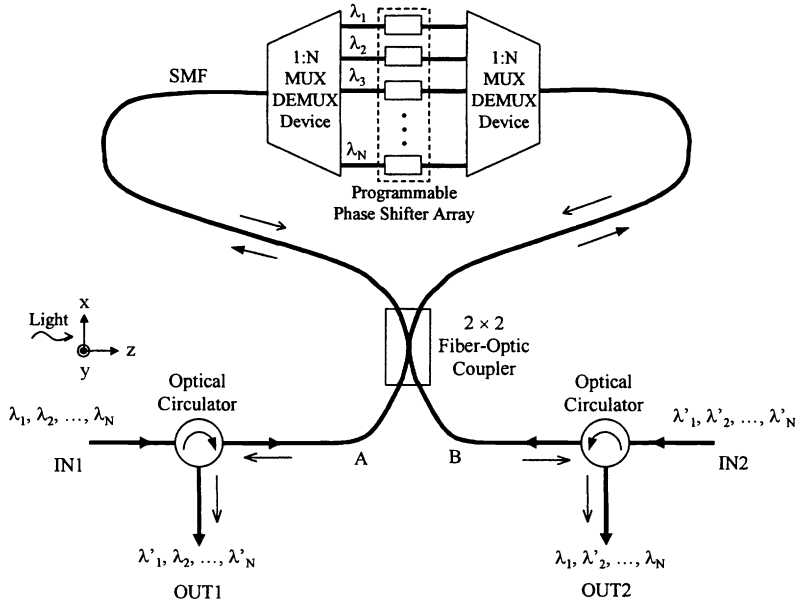

Fig.1 The basic structure of our all-fiber multiwavelength 2 × 2 fiber-optic switch (FOS) structure using a fiber loop mirror (FLM) arrangement.

The basic structure of our FLM-based all-fiber multiwavelength 2 × 2 fiber-optic switch structure is shown in Fig.1. The design uses two three-port optical circulators, a 50:50 2 × 2 fiber-optic coupler, two WDM devices, and an array of programmable phase shifters to form a symmetric multiwavelength 2 × 2 switching structure. The phase shifter controls the phase retardation of the fiber loop and can be a wound fiber around a current carrying conductor to induce the Faraday effect such as used in the optical fiber sensor applications [8] or a polarization insensitive rotatable waveplate [27]. This implies that either a non-reciprocal (e.g., Faraday effect) or reciprocal phase shifter (e.g., rotatable waveplate) can be used in our 2 × 2 FOS structure. As shown in Fig.1, the multiwavelength optical beams from IN1 and IN2 are launched into port A and port B of the 50:50 2 × 2 fiber-optic coupler, respectively, by passing through the three-port optical circulators. For each input optical beam to the coupler, two beams that are counter propagating are generated in the fiber loop. These beams, after passing through the WDM devices and programmable phase shifters interfere at the coupler. Keep in mind that in the

coupler, each time light is coupled across the waveguides, it suffers a $\pi/2$ phase lag with respect to the light traveling straight through in the device [28]. Here, we assume a polarization maintaining loop medium with no birefringence or external influences such as pressure and temperature on the optical fields in the loop. Hence, the clockwise and the anti-clockwise optical fields on recombination at the coupler original input port are in phase and exit at this port. This implies that the multiwavelength optical beams fed to port A and port B of the coupler are sent back to port A and port B, respectively. Now if a π phase shift is generated in the loop, the interfering beams at the coupler are out of phase. In this case, light input from A outputs from B, and light input from B outputs from A. Hence, by inserting a binary 0 or π programmable phase shifter, a 2×2 switch can be formed.

Now consider the loop made of a low cost SMF that can be assumed as a birefringent element. In this case, the unknown fiber loop birefringence produces a variation of optical path length based on the different state of light polarizations (SOPs) of the two beams in the loop. Under these non-ideal switching conditions, some of the light fed at port A and port B of the coupler are transmitted to port B and port A of the coupler, respectively, resulting in switch crosstalk. The ratios of the optical powers at the switch output ports can be described as [6]:

$$P_{out(i)} / P_{in(i)} = R = 4(10^{-2\gamma/10})LK(1-K)|J|^2, \quad (1)$$

and

$$P_{out(j)} / P_{in(i)} = T = (10^{-2\gamma/10})L[1-4K(1-K)|J|^2], \quad (2)$$

where i, j =1 or 2 and $i \neq j$ in eqn(2). Here, $P_{out(i)}$ and $P_{out(j)}$ are the output optical powers at port "i" and "j", respectively. $P_{in(i)}$ is the input optical power at port i. R is the power reflection coefficient, T is the power transmission coefficient, γ is the excess loss of the coupler expressed in decibels, L is the loss due to the optical components inside the fiber loop (e.g., WDM devices, phase shifters, and optical fibers), and K is the coupling ratio of the coupler. $J = \exp(j\phi)\sin^2\theta + \cos^2\theta$ is the Jones matrix element of the fiber loop representing a waveplate that has a phase retardation of ϕ and is orientated at an angle θ with respect to the y axis in a Cartesian coordinate system.

From eqn(1) and eqn(2), it is clear that a binary switch operation can be performed by controlling $|J|$. For instance, when K=0.5, γ=0 dB, and the retardation of the fiber loop is a multiple of 2π (i.e., J=1), R=L and T=0. This implies that the desired wavelength optical beams from IN1 (e.g., λ_2) and IN2 (e.g., λ'_2) show up at OUT1 and OUT2, respectively. On the other hand, when the fiber loop represents a half waveplate with its fast axis orientated at an angle of 45° with respect to the x-y Cartesian coordinate system, J=0, giving R=0 and T=L. In this case, the desired wavelength optical beams from IN1 (e.g., λ'_1) and IN2 (e.g., λ_1) travel to OUT2 and OUT1, respectively. Thus, 2×2 switch operation can be obtained by controlling the retardation of the fiber loop. Note that the optical loss "L" that an output beam suffers can be compensated by using an optical amplifier placed inside or outside the fiber loop.

3. PROPOSED MEMS-BASED POLARIZATION CONTROLLERS

As discussed in section II, the ON-OFF half waveplate is required for our 2×2 FOS and this can be achieved by means of a polarization controller (PC). Since our 2×2 FOS module does not require precise optical alignment due to the use of all fiber-based components, it would be highly desirable to employ fiber-based PCs in our 2×2 FOS structure.

It is well known that strain can cause birefringence change in an optical fiber and therefore a fiber can be applied to implement a PC. When an optical fiber is under the stress applied at 0° with respect to the horizontal or x- axis (i.e., 0° fiber squeezer), the optical field at the optical fiber output can be expressed using the Jones matrix method as:

$$\begin{bmatrix} E_{out,x} \\ E_{out,y} \end{bmatrix} = \begin{bmatrix} \exp[-j\Gamma_1/2] & 0 \\ 0 & \exp[j\Gamma_1/2] \end{bmatrix} \begin{bmatrix} E_{in,x} \\ E_{in,y} \end{bmatrix}, \quad (3)$$

where Γ_1 is the induced phase retardation in the optical fiber. $E_{in,x}$, $E_{in,y}$ and $E_{out,x}$, $E_{out,y}$ are the input and output optical fields in the x and y directions, respectively.

For a 45° fiber squeezer, the output optical field in the x-y Cartesian coordinate system can be written as [29]:

$$\begin{bmatrix} E_{out,x} \\ E_{out,y} \end{bmatrix} = \begin{bmatrix} \cos 45° & \sin 45° \\ -\sin 45° & \cos 45° \end{bmatrix} \begin{bmatrix} \exp[-j\Gamma_2/2] & 0 \\ 0 & \exp[j\Gamma_2/2] \end{bmatrix} \begin{bmatrix} \cos 45° & -\sin 45° \\ \sin 45° & \cos 45° \end{bmatrix} \begin{bmatrix} E_{in,x} \\ E_{in,y} \end{bmatrix},$$

$$\begin{bmatrix} E_{out,x} \\ E_{out,y} \end{bmatrix} = \begin{bmatrix} \cos(\Gamma_2/2) & j\sin(\Gamma_2/2) \\ j\sin(\Gamma_2/2) & \cos(\Gamma_2/2) \end{bmatrix} \begin{bmatrix} E_{in,x} \\ E_{in,y} \end{bmatrix}. \tag{4}$$

Here, Γ_2 is the induced phase retardation in the optical fiber stressed at 45°. By combining the 0° fiber squeezer with the 45° fiber squeezer, the resultant of the output optical field can be found as:

$$\begin{bmatrix} E_{out,x} \\ E_{out,y} \end{bmatrix} = \begin{bmatrix} \cos(\Gamma_2/2) & j\sin(\Gamma_2/2) \\ j\sin(\Gamma_2/2) & \cos(\Gamma_2/2) \end{bmatrix} \begin{bmatrix} \exp[-j\Gamma_1/2] & 0 \\ 0 & \exp[j\Gamma_1/2] \end{bmatrix} \begin{bmatrix} E_{in,x} \\ E_{in,y} \end{bmatrix},$$

$$\begin{bmatrix} E_{out,x} \\ E_{out,y} \end{bmatrix} = \begin{bmatrix} \cos[\Gamma_2/2]\exp[-j\Gamma_1/2] & j\sin[\Gamma_2/2]\exp[j\Gamma_1/2] \\ j\sin[\Gamma_2/2]\exp[-j\Gamma_1/2] & \cos[\Gamma_2/2]\exp[j\Gamma_1/2] \end{bmatrix} \begin{bmatrix} E_{in,x} \\ E_{in,y} \end{bmatrix}. \tag{5}$$

Eqn(5) points out that any input polarized light can be transformed into any desired output polarized light by using 0° and 45° fiber squeezers. However, to achieve endless polarization control, a minimum set of two 0° and two 45° fiber squeezer modules is needed [30]. Endless polarization control implies that any reset of finite range retarders which are used to transform the polarization should cause no temporary incorrect output SOP. Hence, in this paper, we propose to exploit this four-fiber squeezer configuration and combine it with MEMS technology in order to realize a low-cost high-speed and compact fiber-based PC.

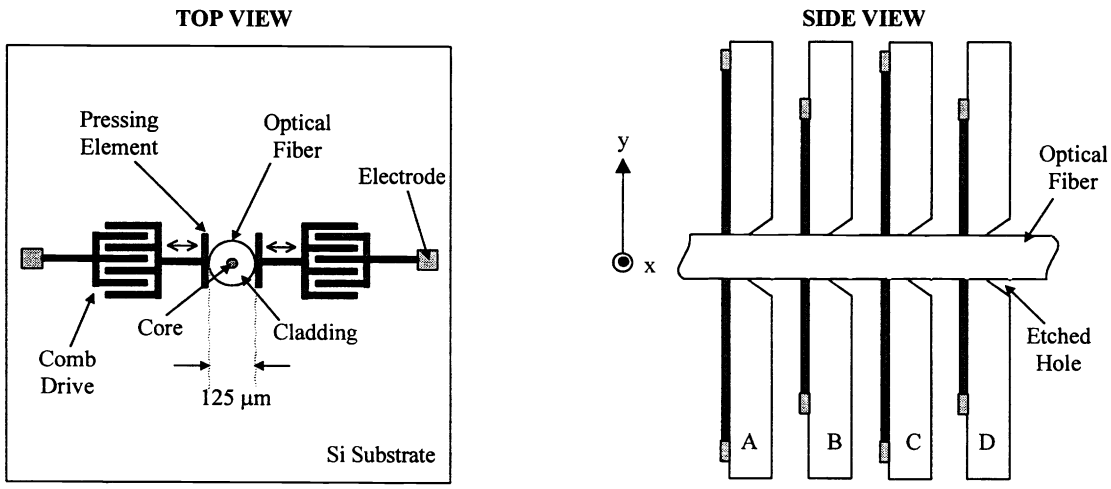

(a) (b)

Fig.2 shows our MEMS-based fiber squeezer: (a) fiber squeezer with the use of electrostatic comb drive actuators and (b) 4-chip arrangement for the implementation of the fiber-based PC.

Fig.2(a) shows our MEMS-based fiber squeezer that utilizes the electrostatic comb drive actuator. The through hole on the Si substrate in which the optical fiber is inserted can be made via the etching process. In this architecture, the fiber is compressed by the two pressing elements when the two comb drive actuators are set to move toward each other. By using four MEMS chips and arranging them at 45° with respect to the adjacent chips (see Fig.2(b)), a MEMS-based PC is accomplished. Note that modules A and C are 0° fiber squeezers while modules B and D are 45° fiber squeezers.

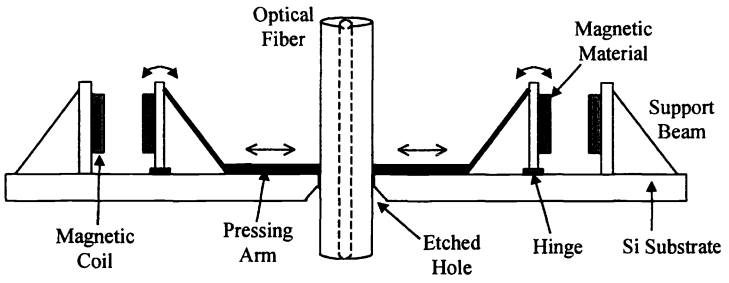

Fig.3 shows our MEMS-based fiber squeezer using magnetic actuators.

Instead of using electrostatic actuation, other actuation techniques such as thermal and magnetic actuators can also be employed. Fig.3 shows our MEMS-based fiber squeezer that exploits the magnetic actuation technique. In this method, the motion of the pressing arms depends upon the magnetic force between the magnetic material (e.g., permalloy) and the magnetic coil. When the magnetic coil is set in such a way that its magnetic polarity is the same as the magnetic material, the magnetic propelling force causes the magnetic material to rotate around the hinge, pushing the pressing arm to move toward the optical fiber. On the other hand, when the magnetic polarity of the magnetic coil is opposite to the polarity of the magnetic material, the pressing arm is moved away from the optical fiber, reducing the pressing force on the optical fiber.

With the use of the magnetic actuation method, the technique based on magnetic levitation (MAGLEV) and propulsion can also be applied. Recently, this technique has been introduced to realize the MEMS-based fiber Bragg grating compressor [31]. Fig.4 manifests our MEMS-based fiber squeezer that takes advantage of MAGLEV and magnetic propulsion principles. In this case, two permanent magnets are located in the rail and are arranged such that their surfaces having the same magnetic polarity are facing each other. One permanent magnet is fixed on the Si substrate while another one is levitating due to the magnetic propelling force. If the magnetic coil located on the one side of the pressing arm is set to have the same magnetic polarity as the floating permanent magnet, the optical fiber will be pressed. Conversely, when the permanent magnet and the magnetic coil have different magnetic polarity, the pressing elements will move away from the optical fiber. In this way, the two stoppers are used to prevent the floating permanent magnet out of the rail.

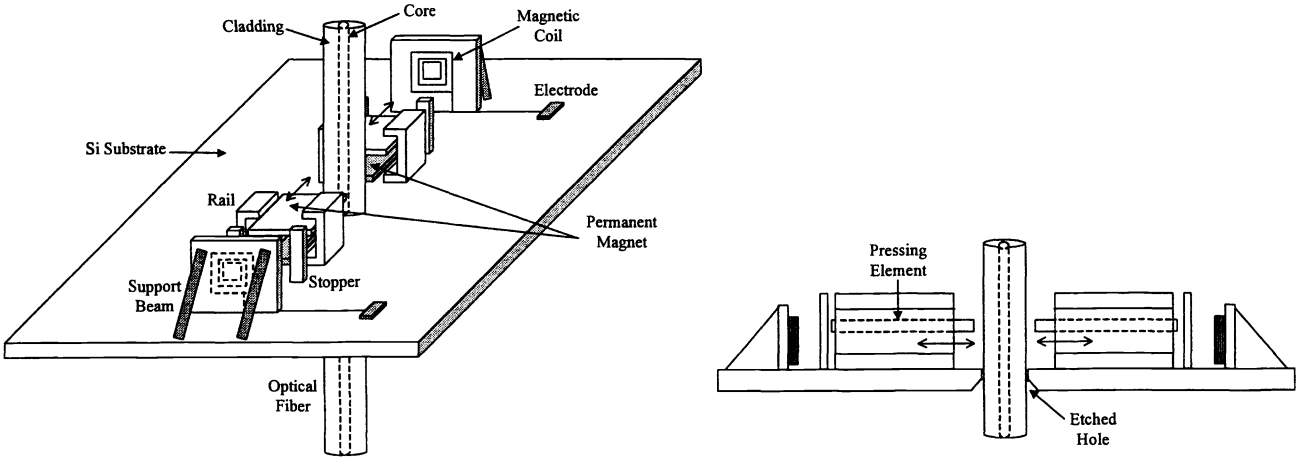

Fig.4 shows the concept of the MEMS-based fiber squeezer with the use of magnetic levitation (MAGLEV) and propulsion technique: (a) perspective view and (b) side view.

Based on the study of pressure on an optical fiber [32], the induced birefringence δ in the unit of rad/m can be expressed as.

$$\delta = (6.03\times10^{-11})[F/(\lambda d)], \quad (6)$$

where, the constant 6.03×10^{-11} rad.m^2/Newton comes from the refractive index, the Poisson's ratio, the Young's modulus, and the strain-optic coefficients of fused silica. F is the line force in Newton/m, λ is the optical wavelength in meters, and d is the fiber diameter in units of meter.

Since the length of the compressing element is equal to the length of the optical fiber which is pressed in order to have the birefringence of δ, the units of F in Newton/m and δ in rad/m can be changed to Newton and rad, respectively. For a typical 125 μm diameter SMF and λ=1550 nm, the calculated compressing force of 20.19 Newtons is needed from each MEMS-based fiber squeezer. However, although this required high force can be obtained with the MEMS-based multi-layered electrostatic film technique [33], it would be desirable to reduce the required compressing force in order to minimize the electrical power consumption. As expressed in eqn(6), one solution is to reduce the diameter of the optical fiber by etching away part of the cladding layer. Fig.5 shows the plot of the required force to achieve δ of 2π rad versus the diameter of the optical fiber, indicating that the required compressing force is reduced when the diameter of the optical fiber decreases.

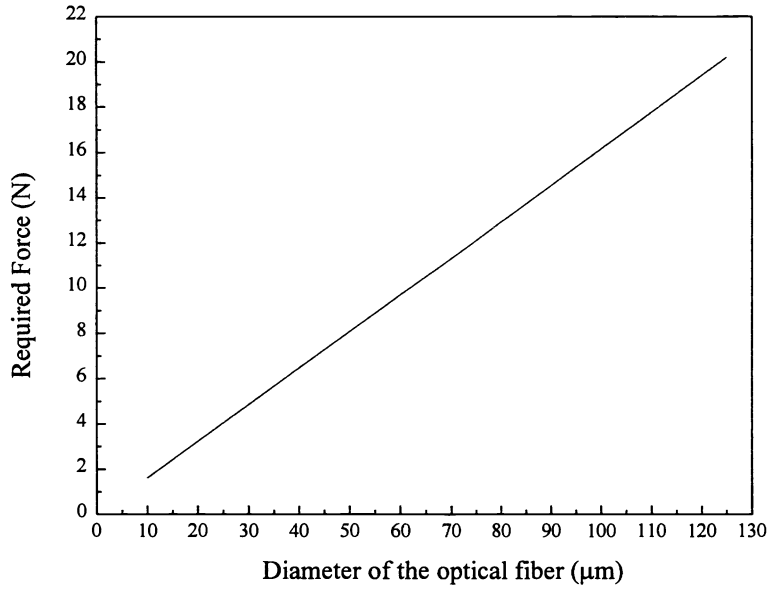

Fig.5 Relationship between the required force to achieve δ of 2π rad and the diameter of the optical fiber.

Another way to reduce the force is to set the required δ per squeezer chip to $2\pi/K$, where K is the number of squeezer chips. In this case, a total number of 4K MEMS chips is needed for the four-squeezer-based PC configuration. With this issue in mind, a MEMS device that has several sets of fiber squeezers rather than one set of squeezers can be used as illustrated in Fig.6. Again, in this case each squeezing element in the MEMS chip provides a δ of $2\pi/K$ rad which in turn reduces the number of required MEMS chips from 4K to 4.

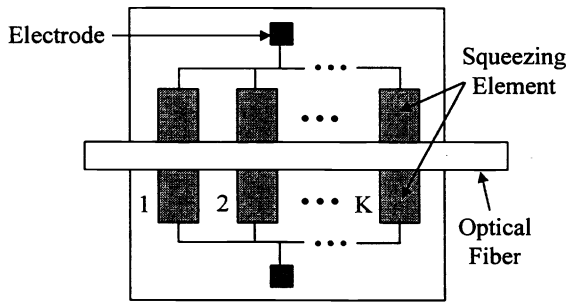

Fig.6 Top view of an array of fiber squeezers arranged in one MEMS chip.

4. EXPERIMENTAL DEMONSTRATION OF THE FLM-BASED ALL-FIBER 2X2 FIBER-OPTIC SWITCH

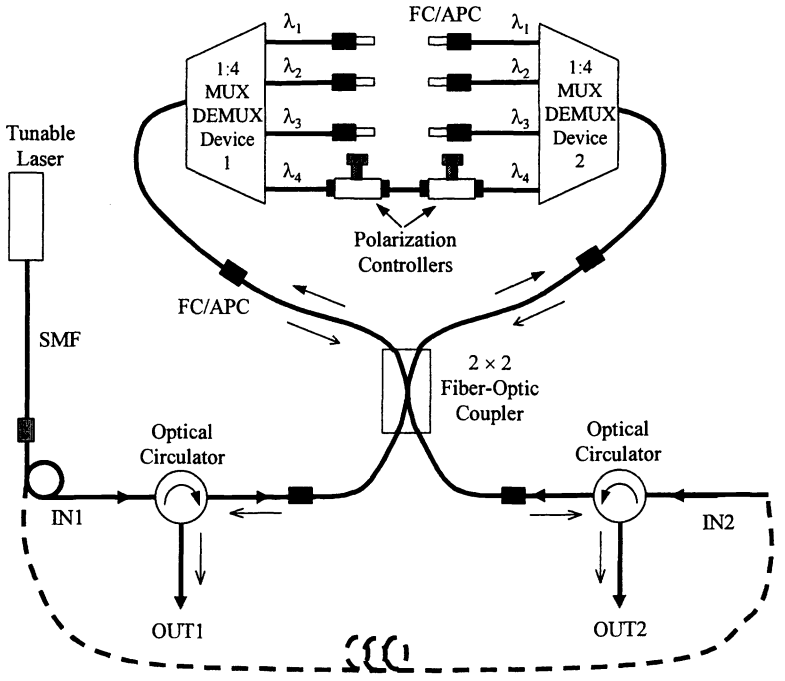

Fig.7 Experimental setup of our FLM-based 4-wavelength 2 × 2 FOS.

The experimental setup of our 2 × 2 FOS is shown in Fig.7. We use a tunable laser diode with a center wavelength of 1550 nm that can provide a uniform 9 mW maximum optical output power from 1540 nm to 1590 nm wavelength. A 2 × 2 fiber-optic coupler with a measured 51.7 : 48.3 coupling ratio at 1550 nm is used. The fiber loop consists of two 4-channel (i.e., λ_1=1546.92 nm, λ_2=1548.52 nm, λ_3=1550.12 nm, and λ_4=1551.72 nm) fiber connectorized WDM devices. One WDM device is based on an array waveguided grating (AWG) and the other one is an interference filter (IF)-based device. The fiber loop length is about 7 m in length. We tested our switch operation one wavelength at a time. Two cascaded mechanical fiber-based PCs are used to form the polarization insensitive programmable waveplate. The two mechanical PCs provide the degrees of freedom to compensate for the unknown birefringence in the loop, thus providing enough phase retardation for a low crosstalk switch. This fiber-based PC is operated via the fiber squeezing and rotating principles. Fiber squeezing process induces the change of the birefringence in the optical fiber whereas the rotating fiber gives the polarization rotation. Note that FC/APC connectors are used for component connections so that the optical noise due to the back reflections in the structure can be ignored. One important system performance issue is optical coherent crosstalk. It is defined as the ratio of the optical noise power for a given wavelength at the unwanted switch output port to the optical signal power from the same wavelength at the desired switch output port. The measured average optical coherent crosstalk in our 2 × 2 FOS is -31.2 dB. Another important system issue is the optical loss that is the ratio of the optical power fed into our switch structure to the optical power at the desired switch output port. An average optical loss of 20.76 dB is measured for our 2 × 2 FOS, limited by the AWG-based WDM device (10.05 dB), the IF-based WDM device (7.29 dB), and two three-port optical circulators (1.21 dB). In addition, other losses are the 0.14 dB total excess loss of the coupler (i.e., for γ=0.07 dB, total excess loss "2γ"=0.14 dB), the two PCs (0.37 dB), and the four fiber adapters (1.70 dB).

PDL is also an important issue for a switch. In this case, the fiber outside the loop is twisted and pressed so that the SOP of the input optical beam to the switch is varied. The measured average PDL of our switch structure is 0.75 dB, limited by the present high 0.2 dB PDL of the IF-based WDM device and 0.5 dB PDL of AWG-based WDM device used in our structure. In fact, the measured average PDL of the switch structure without the multiplexers is 0.08 dB within a 50 nm bandwidth, limited by the PDL of the three-port optical circulators and the coupler used in our experimental setup. This very low 0.08 dB PDL value clearly implies that the 0.75 dB PDL measured in our 4-channel switching test with the multiplexers is caused

by our WDM devices. Hence, inherently our switch structure has very low PDL as required by commercial optical communication applications.

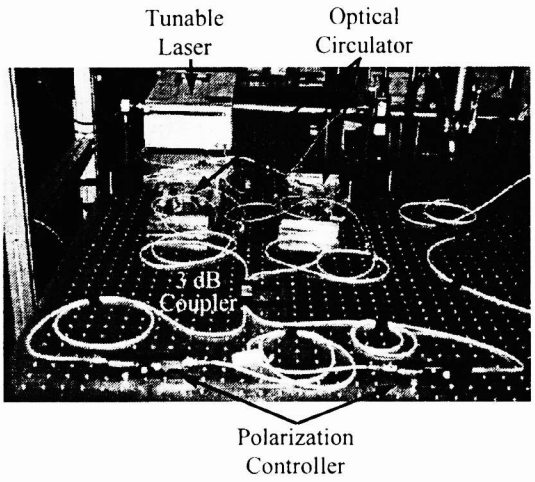

Fig.8 Photograph of our FLM-based 2 × 2 FOS experimental demonstration for the broadband operation test.

To observe broadband switch operation, the WDM devices are removed from the fiber loop as shown in Fig.8. This time, the fiber loop length is about 3 m, again implying a much lower cost compared to a > 1 km long DSF used in the NLM-based fiber-version structures.

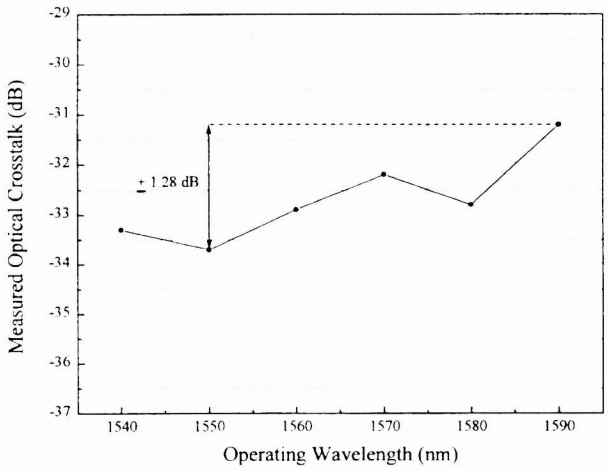

Fig.9 The measured optical coherent crosstalk versus the operating wavelength for the broadband switch operation test.

Fig.9 shows the plot of the measured optical coherent crosstalk over a 50 nm bandwidth, indicating an average optical coherent crosstalk of -32.7 dB with a fluctuation of ± 1.28 dB. Using eqn(1) and eqn(2) with the measured coupling ratio (e.g., 51.7 : 48.3) mentioned earlier, the normalized optical powers at port "i" and port "j" for the optical beam input at port "i" are 4(0.483)(1-0.483) = 0.998844 and 1-0.998844 = 0.001156, respectively. This indicates an optical coherent crosstalk of $10log(0.001156/0.998844) = -29.4$ dB. Hence, the optical coherent crosstalk of our 2 × 2 FOS structure is limited by the coupling ratio of the 3 dB fiber-optic coupler used in the experiment. With a commercial broadband 50:50 2 × 2 coupler that has a splitting ratio fluctuation of ± 1.75% over a 60 nm bandwidth [34], the average optical coherent crosstalk of -29.1 dB is calculated. This shows that our 2 × 2 FOS structure is practical for the WDM systems.

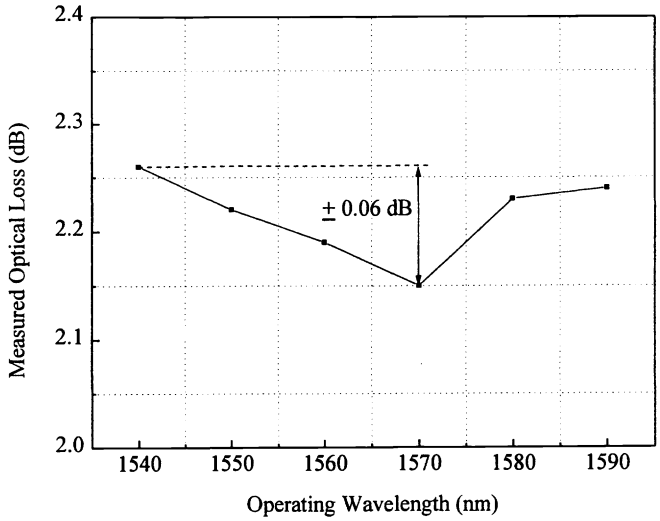

Fig.10 The measured optical loss versus the operating wavelength for the broadband switch operation test.

The measured optical loss versus operating wavelength is plotted in Fig.10, indicating an average optical loss of 2.22 dB with a loss fluctuation of ± 0.06 dB. This optical loss value comes from two three-port optical circulators (1.21 dB), two PCs (0.37 dB), fiber adapters (0.50 dB), and the total excess loss of the coupler (0.14 dB). This data also indicates that our switch structure is inherently low loss if low loss WDM devices are used for multiwavelength switching.

5. CONCLUSION

An all-fiber FLM-based multiwavelength 2 × 2 FOS has been proposed using simple polarization control. A polarization insensitive programmable waveplate effect rather than the nonlinear optical effect in the fiber is used to achieve a symmetric 2 × 2 switch design. This design change leads to short fiber lengths and low laser power overhead for the switch. Experimental results from a four-wavelength switch indicates an average optical coherent crosstalk of –31.2 dB. The measured average optical loss in our multiwavelength switch structure is 20.76 dB, limited mainly by the two WDM devices. Without WDM devices, a 50 nm broadband switch operation is investigated, giving a measured average optical loss of 2.22 dB with a loss fluctuation of ± 0.06 dB. In this case, the measured average optical coherent crosstalk is –32.7 dB with a ± 1.28 dB fluctuation, limited by the imperfection (i.e., non 50:50 split) of the 3 dB fiber-optic coupler used in the structure. An average PDL of 0.08 dB is measured for our switch without the multiplexers. FOS speed is determined by the speed of the PC device, and can range from milliseconds for NLC-based [28] and MEMS-based architectures to microseconds for integrated optics-based structure [35]. If needed, the ultimate faster switching speed can be realized with the NLM effect within our multiwavelength switch structure, although at the cost of high switch complexity. Future work relates to the design optimization and experimental demonstration of the fiber-based PC using our proposed MEMS-based fiber squeezer modules.

REFERENCES

[1] M. S. Borella, J. P. Jue, B. Ramamurthy, and B. Mukherjee, "Optical components for WDM lightwave networks," *Proc. IEEE* **85**, pp. 1274-1307, 1997.

[2] R. A. Soref, "Low-crosstalk 2 × 2 optical switch," *Opt. Lett.* **6**, pp. 275-277 1981.

[3] N. A. Riza and S. Yuan, "Low optical interchannel crosstalk, fast switching speed, polarization independent 2 × 2 fiber optic switch using ferroelectric liquid crystals," *Electron. Lett.* **34**, pp. 1341-1342, 1998.

[4] N. A. Riza and D. L. Polla, "Microdynamical fiber-optic switch," *U.S. Patent*, 5208880, May 4, 1993.

[5] C. Marxer and N. F. de Rooij, "Micro-op-mechanical 2 × 2 switch for single-mode fibers based on plasma-etched silicon mirror and electrostatic actuation," *J. of Lightwave Technol.* **17**, pp. 2-6, 1999.

[6] D. B. Mortimore, "Fiber loop reflectors," *J. of Lightwave Technol.* **6**, pp. 1217-1988, 1988.

[7] N. J. Doran and D. Wood, "Nonlinear-optical loop mirror," *Opt. Lett.* **13**, pp. 56-58, 1988.

[8] J. Blake, P. Tantaswadi, R. T. de Carvalho, "In-line Sagnac interferometer current sensor," *IEEE Trans. Power Delivery* **11**, pp. 116-121, 1996.
[9] A. Huang, N. Whitaker, H. Avramopoulos, P. French, H. Hough, and I. Chuang, "Sagnac fiber logic gates and their possible applications: a system perspective," *Appl. Opt.* **33**, pp. 6254-6267, 1994.
[10] Y. Chai, J. H. Chen, F. S. Choa, J. P. Zhang, J. Y. Fan, and W. Lin, "Scalable and modularized optical random-access memories for optical packet-switching networks," *CLEO'98*, p. 397, 1998.
[11] H. C. Lim, F. Futami, and K. Kikuchi, "Polarization-independent, wavelength-shift-free optical phase conjugator using a nonlinear fiber Sagnac interferometer," *IEEE Photon. Technol. Lett.* **11**, pp. 578-580, 1999.
[12] J.-X. Cai, K.-M. Feng, X. P. Chen, and A. E. Willner, "Equalization of nonuniform EDFA gain using a fiber-loop mirror," *IEEE Photon. Technol. Lett.* **9**, pp. 916-918, 1997.
[13] X. Fang and R. O. Claus, "Polarization-independent all-fiber wavelength-division multiplexer based on a Sagnac interferometer," *Opt. Lett.* **20**, pp. 2146-2148, 1995.
[14] E. A. Swanson and J. D. Moores, "A fiber frequency shifter with broad bandwidth, high conversion efficiency, pump and pump ASE cancellation, and rapid tunability for WDM optical networks," *IEEE Photon. Technol. Lett.* **6**, pp. 1341-1343, 1994.
[15] I. Glesk, J. P. Sokoloff, and P. R. Prucnal, "Demonstration of all-optical demultiplexing of TDM data at 250Gbit/s," *Electron. Lett.* **30**, pp. 339-341, 1994.
[16] D. A. Pattison, P. N. Kean, W. Forysiak, I. Bennion, and N. J. Doran, "Bandpass switching in a nonlinear-optical loop mirror," *Opt. Lett.* **20**, pp. 362-364, 1995.
[17] R. J. Manning, A. E. Kelly, A. J. Poustie, and K. J. Blow, "Wavelength dependence of switching contrast ratio of semiconductor optical amplifier-based nonlinear loop mirror," *Electron. Lett.* **34**, pp. 916-918, 1998.
[18] J. W. Lou, T. J. Xia, Y. Liang, Y.H. Kao, O. Boyraz, K. H. Ahn, and M. N. Islam, "All-optical TDM add/drop multiplexer demonstration with 100-Gbits/s words," *CLEO'98*, pp. 3-4, 1998.
[19] Wave Optics, Inc., Product Catalog, 1999.
[20] B.-E. Olsson, N. Lagerqvist, A. Boyle, and P. A. Andrekson, "Elimination of acoustic sensitivity in nonlinear optical loop mirrors," *J. of Lightwave Technol.* **17**, pp. 343-346, 1999.
[21] Y. Liang, J. W. Lou, J. K. Andersen, J. C. Stocker, O. Boyraz, and M. N. Islam, "Polarization-insensitive nonlinear optical loop mirror demultiplexer with twisted fiber," *Opt. Lett.* **24**, pp. 726-728, 1999.
[22] K. Uchiyama, H. Takara, S. Kawanishi, T. Morioka, and M. Saruwatari, "Ultrafast polarization-independent all-optical switching using a polarization diversity scheme in the nonlinear optical loop mirror," *Electron. Lett.* **28**, pp. 1864-1866, 1992.
[23] B.-E. Olsson and P. A. Andrekson, "Polarization independent demultiplexing in a polarization diversity nonlinear optical loop mirror," *IEEE Photon. Technol. Lett.* **9**, pp. 764-766, 1997.
[24] *TR-NWT-001073: Generic Requirements for Fiber Optic Switches*, Bellcore, Issue 1, January 1994.
[25] S. Sumriddetchkajorn and N. A. Riza, "Fiber-connectorized multiwavelength 2x2 switch structure using a fiber loop mirror," *Opt. Commun.* **175**, pp. 89-95, 2000.
[26] Patent Pending
[27] Y. Ohtera, T. Chiba, and S. Kawakami, "Liquid crystal rotatable waveplates," *IEEE Photon. Technol. Lett.* **8**, pp. 390-392, 1996.
[28] S. Lacroix, F. Gonthier, and J. Bures, "Modeling of symmetric 2 × 2 fused-fiber couplers," *Appl. Opt.* **33**, pp. 8361-8369, 1994.
[29] R. Noé, H. Heidrich, and D. Hoffmann, "Endless polarization control systems for coherent optics," *J. Lightwave Technol.* **6**, pp. 1199-1208, 1988.
[30] N. G. Walker and G. R. Walker, "Endless polarisation control using four fibre squeezers," *Electron. Lett.* **23**, pp. 290-292, 1987.
[31] N. A. Riza and S. Sumriddetchkajorn, "Micromechanics-based wavelength-sensitive photonic beam control architectures and applications," *Appl. Opt.* **39**, pp. 919-932, 2000.
[32] A. M. Smith, "Single-mode fibre pressure sensitivity," *Electron. Lett.* **16**, pp. 773-774, 1980.
[33] T. Niino, S. Egawa, H. Kimura, and T. Higuchi, "Electrostatic artificial muscle: compact, high-power linear actuators with multiple-layer structures," *Proc. IEEE MEMS*, pp. 130-135, 1994.
[34] Gerald Curtin, Applications Engineer, E-TEK Dynamics, Inc., 1865 Lundy Avenue, San Jose, California, USA., Private Communication, 1999.
[35] F. Heismann, "Analysis of a reset-free polarization controller for fast automatic polarization stabilization in fiber-optic transmission systems," *J. of Lightwave Technol.* **12**, pp. 690-699, 1994.